



Biosorption of methylene blue from aqueous solution by potato (*Solanum tuberosum*) peel: equilibrium modelling, kinetic, and thermodynamic studies

El-Khamssa Guechi*, Oualid Hamdaoui

Laboratory of Environmental Engineering, Faculty of Engineering, Department of Process Engineering, Badji Mokhtar - University, P.O. Box 12, 23000 Annaba, Algeria, emails: guichi_wahida@yahoo.fr (E.-K. Guechi), ohamdaoui@yahoo.fr (O. Hamdaoui)

Received 13 April 2014; Accepted 22 March 2015

ABSTRACT

In this study, an abundant agricultural waste, potato (*Solanum tuberosum*) peel, was used as a biosorbent material to test its suitability for removing a basic dye, methylene blue (basic blue 9), from aqueous solutions. The potato peel (PP) was characterized by infrared spectroscopy (FTIR), specific surface area, isoelectric potential (pH_{ZPC}), and scanning electron microscopy and the functional organic groups were determined by the Boehm titration method. The influence of operating conditions such as contact time, initial concentration of the dye, biosorbent dose, ionic strength, initial solution pH, temperature, and biosorbent particle size on dye removal was discussed. The results show that the increase of the initial concentration, dose of biosorbent material, and pH has a positive impact on the biosorption of dye. However, the ionic strength, the temperature, and particle size have a negative effect on the dye removal. Biosorption kinetic data obtained at different concentrations were modeled using the Lagergren's pseudo-first-order and Blanchard's pseudo-second-order kinetic models to determine the rate constants. It was found that the kinetics of the biosorption of dye closely followed the pseudo-second-order kinetic model. Equilibrium biosorption data were analyzed by four isotherms, namely the Langmuir isotherm, the Freundlich isotherm, the Elovich isotherm, and the Flory–Huggins isotherm. The equilibrium data were best represented by the Langmuir isotherm model, showing maximum monolayer biosorption capacity, q_m , of 105.26 mg g^{-1} . It can be concluded that the PP has homogeneous surface energy. Thermodynamic parameters such as standard enthalpy change (ΔH°), standard entropy change (ΔS°), and standard free energy change (ΔG°) were evaluated. The thermodynamic results suggest that the biosorption is a typical physical process, spontaneous, and exothermic in nature.

Keywords: Biosorption; Methylene blue; Potato peel; Characterization; Isotherm; Modeling

1. Introduction

Among the different pollutants of aquatic ecosystem, dyes are a large and important group of

chemicals. It is reported that there are over 100,000 commercially available dyes with a production of over 7×10^5 metric tonnes per year [1,2]. They are widely used in industries such as textiles, paper, rubber, plastics, cosmetics, etc. These dyes are left in the industrial wastes and consequently discharged mostly

*Corresponding author.

in surface water resources. Dyes even in low concentrations are visually detected, and affect the aquatic life and food chain. These colored compounds are not only esthetically displeasing but also inhibiting sunlight into the stream and reducing the photosynthetic reaction. Due to the large degree of organic compound in these molecules and the stability of modern dyes, conventional physicochemical and biological treatment methods are ineffective for their removal [3]. Recently, the principal existing and emerging processes for dyes removal have been compiled by Crini [4]. Since many organic dyes are harmful to human beings, the removal of methylene blue (MB) is not regarded as acutely toxic, but it can have various harmful effects. When inhaled, it can give rise to short periods of rapid or difficult breathing, while ingestion through the mouth produces a burning sensation and may cause nausea, vomiting, diarrhea, and gastritis. A large amount creates abdominal and chest pain, severe headache, profuse sweating, mental confusion, painful micturation, and methemoglobinemia-like syndromes [5]. The conventional methods, such as coagulation and flocculation, used for the removal of dyes from water introduce metallic impurities and produce a large amount of sludge which requires further disposal. The sludge-free treatments are, therefore, gaining importance. Activated carbon adsorption is of one such method which has a great potential for the removal of dyes from wastewater [3,6–10]. However, they are not always well known as they are not economically viable and technically efficient.

Among the numerous treatment technologies developed for the removal of dyes from industrial effluents, biosorption is an attractive and promising technology. The study of biosorption is of great importance from an environmental point of view, as it can be considered as an alternative technique for removing toxic pollutants from wastewaters [11–13]. Undoubtedly, agricultural waste biomass is currently one of the most challenging topics, which have been gaining considerations over the last decades. In perspective, potato peel (PP) has emerged to be an invaluable source.

Potato (*Solanum tuberosum*) peel is an herbaceous perennial of the Solanaceae family. It is an easily available waste that could be an alternative for costly wastewater treatment processes. Losses caused by potato peeling range from 15 to 40% which depends on the procedure used, i.e. steam, abrasion or lye peeling. Chemical composition of a potato contains 70 to 80% water, carbohydrates including starch, proteins, and mineral elements as P, Ca, and Na. Potatoes are peeled as a part of the production of

French fries, crisps, puree, instant potatoes, and similar products. The produced waste is 90 kg per Mg of influent potatoes and is apportioned to 50 kg of potato skins, 30 kg starch, and 10 kg inert material. The problem of the PP management causes considerable concern to the potato industries, thus implying the need to identify an integrated, environmentally-friendly solution [14].

For this reason, the PP was proposed as a novel low-cost biosorbent to remove malachite green [14] and MB [15]. However, the latter does not include some characteristics of the PP, and the effect of some kinetic parameters such as temperature, particle size, ionic strength, biosorbent dose. Additionally, the thermodynamic parameters were not investigated. Subsequently, the aim of this study is to investigate and complete what has not been studied in these works. Also, the biosorption parameters obtained using the present biosorbent will be compared with the ones presented in the literature.

2. Materials and methods

2.1. Sorbate

The basic dye used in this study is MB purchased from Sigma–Aldrich. The MB (basic blue 9) was chosen in this study because of its known strong biosorption onto solids. The maximum absorption wavelength of this dye is 664 nm. The structure of MB is shown in Fig. 1. For pH adjustments, analytically pure HCl and NaOH, purchased from Prolabo, were used. Initial pH of dye solutions was around 6 before biosorbent addition. Three hundred milligram per liter stock solution was prepared by dissolving the required amount of dye in distilled water. Working solutions of the desired concentrations were obtained by the successive dilutions.

2.2. Preparation and characterization of biosorbent

The PP used in the present study was obtained from the university canteen. It was washed, dried,

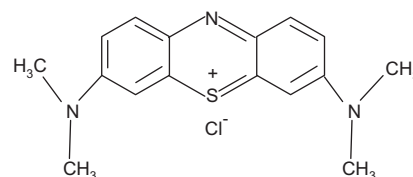


Fig. 1. Chemical structure of MB.

crushed, and sieved to desired mesh size (0.5–1.25 mm). Finally, the obtained material was then dried in an air circulating oven at 50°C for 7 d and stored in a desiccators until use [14]. Principle characteristics of the PP were determined and the results are summarized in Tables 1 and 2.

For the main functional groups that might be involved in dye biosorption, a Fourier transform infrared (SHIMADZU FTIR-8400S) analysis was done on the PP to determine the surface functional groups, and the spectra were recorded from 4,000 to 400 cm⁻¹. Moreover, the concentrations of acid and basic (organic) functional surface groups present on PP were determined by the Boehm titration method. The point of zero charge (pHpzc) of a biosorbent is a very important characteristic that determines the pH at which the biosorbent surface has electrical neutrality. At this value, the acid or basic functional groups no longer contribute to the pH of the solution. The specific surface area (SSA) of PP was determined using an alternative method to the Bruner–Emmet–Teller (BET) method. In addition, the investigation of surface morphology of PP sample before and after biosorption was observed by scanning electron microscopy (SEM).

2.3. Biosorption studies

The batch biosorption experiments were carried out in 150 mL flasks where 0.20 g of the biosorbent was added to 100 mL of the MB solutions at initial concentrations that varied in the range of 10–40 mg L⁻¹. The flasks were placed in a thermostatic water bath to maintain a constant temperature (25°C) and were stirred at 200 rpm for 300 min to ensure that equilibrium was achieved. Aqueous samples (2.5 mL) were taken from each of the MB solutions at preset time intervals (0–300 min) using syringes and the concentrations were then analyzed. The samples were reintroduced after analysis so that the volume of the solution remained constant during the course of the kinetics. The concentrations of MB in the supernatant solution before and after biosorption were determined

Table 1
Principal characteristics of PP

Porosity (%)	74.15
Apparent specific gravity	0.23
Absolute specific gravity	0.89
Mean diameter (mm)	≤2
Point of zero charge (pHpzc)	5.7

Table 2
Chemical composition of PP

Component	Content (%)
Cellulose	50.89
Hemicellulose	21.53
Lignin	19.25
Extractable matters	5.86
Ashes	1.89
Other	0.58

using a double beam UV–Vis spectrophotometer at the maximum wavelength (664 nm). Each experiment was duplicated under identical conditions. The biosorption amount at time t , q_t (mg g⁻¹), and the percentage of dye removal of dye (%R) can be calculated by the following equations:

$$q_t = \frac{(C_0 - C_t)V}{W} \quad (1)$$

$$\%R = \frac{(C_0 - C_t)}{C_0} \times 100 \quad (2)$$

where C_0 and C_t (mg L⁻¹) are the liquid-phase concentrations of dye at initial and at time t , respectively. V is the volume of the solution (L) and W is the mass of dry biosorbent (g).

For isotherm studies, a series of flasks containing 50 mL of MB solution in the range of 40–400 mg L⁻¹ were prepared. The weighed amount of 0.1 g of PP was added to each flask and then the mixtures were agitated at 200 rpm and at constant temperature of 25, 35, or 45°C for 600 min to ensure that equilibrium was reached for the higher concentrations. These experiments were carried out at a natural pH. The amount of biosorption at equilibrium, q_e (mg g⁻¹), was calculated by:

$$q_e = \frac{(C_0 - C_e)V}{W} \quad (3)$$

where C_e (mg L⁻¹) is the liquid-phase concentration of MB dye at equilibrium.

3. Results and discussion

3.1. Characterization of the biosorbent

FTIR spectrum for the waste PP is shown in Fig. 2. It can be seen that a strong peak at 3,450 cm⁻¹ represents the –OH stretching of phenol group of cellulose

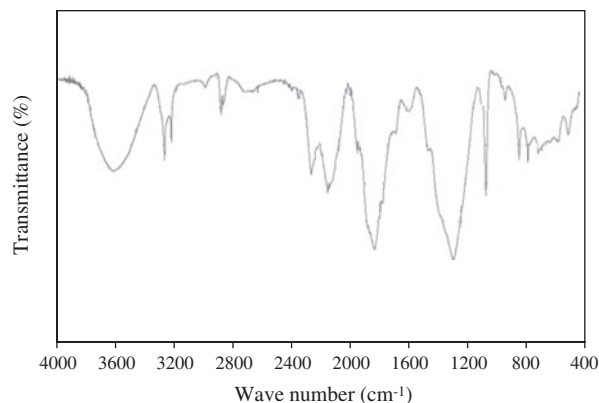


Fig. 2. FTIR spectrum of PP.

and lignin, and a peak at $2,930\text{ cm}^{-1}$ corresponds to $-\text{CH}$ and $-\text{CH}_2$ stretching of aliphatic compound. The peaks at $1,735$ and $1,636\text{ cm}^{-1}$ were attributed to $\text{C}=\text{O}$ stretching of aldehyde group and $\text{C}=\text{C}$ stretching of phenol group, respectively [16]. The peaks at $1,507$, $1,370$, 892 , and 660 cm^{-1} in the spectrum of PP, respectively, can be assigned to $\text{N}-\text{H}$ deformation, $\text{C}-\text{O}-\text{H}$ bend, $\text{C}-\text{N}$ stretch, and $\text{C}-\text{O}-\text{H}$ twists [17]. It is clear that the biosorbent displays a number of biosorption peaks, reflecting the complex nature of the biomaterial.

The traditional Boehm titration method uses a pH-metric titration (chemical method) to identify oxygen (acid and basic) surface groups on the PP [18]. This method is based on the principle that oxygen groups on the surface have different acidities which can be neutralized by bases of different strengths. Each sample of biosorbent (1.00 g) was accurately weighed and mixed with 50 ml of 0.1 N solution of sodium carbonate (Na_2CO_3), sodium bicarbonate (NaHCO_3), sodium hydroxide (NaOH), and sodium ethanolate (NaOC_2H_5) or chlorhydric acid (HCl) in 100 ml flasks. The suspensions of flasks were agitated (140 rpm) at room temperature and it was left for 72 h. Afterwards, the excess of basic and acid (a sample of 10 mL) was filtered and titrated with 0.1 N HCl or 0.1 N NaOH solutions. Acid and basic concentrations were calculated on the basis of the assumption that NaHCO_3 neutralizes the carboxylic groups only, Na_2CO_3 neutralizes the carboxylic and lactonic groups, NaOC_2H_5 neutralizes the carbonylic and quinonic groups, NaOH neutralizes all acidic groups including phenolic groups, and HCl neutralizes all basic groups.

The concentrations of acid and basic groups of PP surface measured by the Boehm titration are shown in Table 3. These results prove that acid sites, the

carboxylic, the carbonylic, and the quinonic groups were the dominant acidic oxygenated groups. And the total acid groups were higher than the total basic groups.

The zero-point charge (pH_{pzc}) of the PP characteristics was calculated using the addition solid method [19]. The initial pH (pH_i) of the prepared KNO_3 solution (0.1 M) was adjusted between 2 and 12 by adding 0.1 N HCl or 0.1 N NaOH solutions. Then, 1 g of PP was added to each flask and the samples were stirred at 140 rpm for 48 h; when equilibrium was established, the final pH (pH_f) of the solutions was measured. The value of pH_{ZPC} can be determined from the curve that crosses the initial pH value lines of the plot ΔpH ($\text{pH}_f - \text{pH}_i$) vs. pH_i . This method was found to be similar to that studied by some authors [20–25]. The result for experimental determination of pH_{ZPC} was found to be 5.7 and is noted above in Table 1.

The SSA is the accessible area of biosorbent surface per unit mass of material. The interference by the surrounding phase, can modify the surface area, is especially problematic for the BET N_2 adsorption/desorption isotherm method because the entire surface is modified by vacuum treatment before N_2 adsorption [26]. As an alternative to the BET method, the SSA ($\text{m}^2\text{ g}^{-1}$) of the PP uses the following equation:

$$\text{SSA} = \frac{F \cdot q_m \cdot N_{\text{AV}} \cdot A}{\text{MW} \times 10^3} 10^{-20} \quad (4)$$

where F is the fraction dye in the commercial product, q_m is the monolayer capacity from Langmuir model (g dye/g solid), N_{AV} the Avogadro number (6.022×10^{23} molecules mol^{-1}), A is the molecular area of the dye (m^2), and MW is the molecular weight of the dye (373.9 g mol^{-1}). The molecular area of MB was taken as 130 \AA^2 [27].

The SSA of PP was found as 167.41, 159.07, and $147.25\text{ m}^2\text{ g}^{-1}$, according to Eq. (4), for the temperatures of 25, 35, and 45°C , respectively. The values of SSA at all the three temperatures was found to be higher compared to that of the other biosorbents which have been studied and where no thermal or chemical treatment was applied [15,26,28–34]. This method has been already used to determine the SSA by some authors in the sorption of dyes and metals on many natural substances such as oil palm trunk fiber [26], banana stem [27], Luffa cylindrical fibers [29], Peat [30], Hazelnut shells and wood sawdust [31], cotton [35], sludge ash [36], and spruce wood [37].

Table 3

Concentration of acid and basic groups on surface PP

Concentration groups	Carboxylic	Lactonic	Phenolic	Carbonylic and quinonic	Acid	Basic	Total
Value (meq g ⁻¹)	1.00	0.009	0.381	0.859	2.249	0.351	2.60

As it is known, SEM is one of the most widely used surface diagnostic tools. Subsequently, Fig. 3(a) and (b) show the SEM of PP sample before and after biosorption of the dye, respectively. The PP (Fig. 3(a)) exhibits a heterogeneous or rough and porous (caves) surface structure which enhanced the biosorption of MB dye.

3.2. The influence of operating conditions

3.2.1. Effect of initial dye concentration and contact time

In order to study the effect of the initial concentration and contact time of MB in the solutions on the biosorption rate by PP, the experiments were carried out at a fixed biosorbent dose (0.20 g), natural pH

(6.2), temperature of 25°C, and at different initial dye concentrations (from 10 to 40 mg L⁻¹) for different time intervals (0–300 min). Fig. 4 shows the effect of the initial dye concentration and contact time on the biosorption of MB by PP. For the different concentrations tested, it can be observed that the biosorption capacity increased with time and reached a constant value where no more MB dye was removed from the solution. Also, it can be seen that the biosorption of MB at different concentrations is rapid in the initial stages and gradually decreases with the biosorption progress until the equilibrium is reached. The initial rate of biosorption was greater for higher initial MB concentration, because the resistance to the dye uptake decreased as the mass-transfer driving force increased. It was noticed that an increase in initial dye concentration led to an increase in the biosorption capacity of MB by PP. The amount of MB biosorbed at equilibrium increased from 3.62 to 14.83 mg g⁻¹ as the concentration was increased from 10 to 40 mg L⁻¹, respectively. Additionally, Fig. 4 shows that the contact time required to reach the equilibrium at initial concentrations from 10 to 40 mg L⁻¹ is from 20 to 75 min, respectively. However, the experimental data were measured at 300 min to make sure that full equilibrium was attained. The kinetic results showed that the curves of contact time are single and continuous leading to equilibrium. These curves indicate the possible monolayer coverage of dye on the surface of

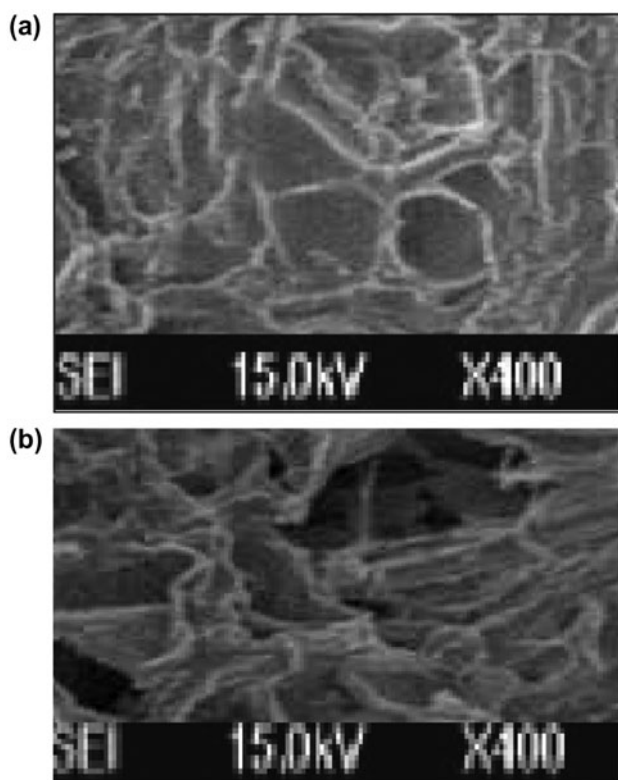


Fig. 3. SEM micrograph of PP before; (a) and after; (b) biosorption of MB dye.

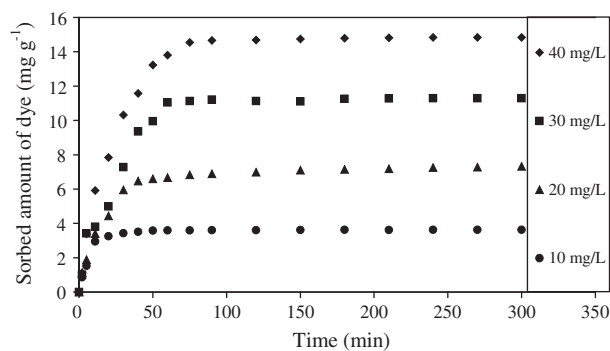


Fig. 4. Kinetics of MB biosorption by PP for various initial dye concentrations (conditions: biosorbent dosage = 0.2 g (100 mL)⁻¹; stirring speed = 200 rpm; T = 25°C; pH 6.2).

PP [14]. A similar phenomenon was observed for the biosorption of MB dye on phoenix tree's leaves [38], wheat shells [39], and castor seed shells [40]. Hameed et al. [41] have further studied the adsorption of MB on garlic peels at initial concentration of 50 mg L^{-1} and have reported that the equilibrium was reached in 90 min. Senthilkumaar et al. [42] have studied the sorption of MB on jute fiber carbon at various concentrations (50, 100, 150, and 200 mg L^{-1}) and have reported that the equilibrium was established at 250 min for all the concentrations studied.

3.2.2. Effect of solution pH

The experiments were carried out at 40 mg L^{-1} initial dye concentration, 0.2 g biosorbent mass, and temperature of 25°C for a contact time of 100 min to ensure that full biosorption equilibrium was attained. However, in reality, equilibrium time was 75 min at this initial dye concentration. These experiments were conducted at different pH values in the range of 2–9 and the solution pH was adjusted using 0.1 N HCl or 0.1 N NaOH aqueous solutions. Fig. 5 shows the effect of pH on the biosorption of MB by PP. It can be seen that there is a decrease in the biosorption with a decrease in pH. The lowest dye biosorption was recorded at pH 2. The amount of MB biosorbed at equilibrium, q_e , increases from 3.79 to 15.77 mg g^{-1} as an increase in pH from 2 to 9, respectively. The influence of the solution pH on the dye uptake can be explained on the basis of the zero-point charge, pH_{zpc} , of the biosorbent. Cation biosorption on any biosorbent will be favorable at $\text{pH} > \text{pH}_{\text{zpc}}$. The surface of the biosorbent becomes negatively charged and favors uptake of cationic dyes due to increased

electrostatic force of attraction. Thus, MB biosorption by PP is favored at higher pH (values higher than pH_{zpc} , 5.7). At lower pH ($\text{pH} < \text{pH}_{\text{zpc}}$), biosorbent surface is positively charged, the concentrations of H^+ were high and they compete with positively charged MB cations for vacant biosorption sites causing a decrease in dye uptake. Similar trends were observed for the biosorption of MB on guava leaf powder [21], wheat shells [39], and rice husk [43].

3.2.3. Effect of temperature

Temperature is one of the most important factors that affect the biosorption rate and dye uptake. The effect of temperature on the biosorption of MB was studied by contacting 0.20 g of biosorbent with 100 mL of dye solution of 40 mg L^{-1} initial concentration. The flasks were placed in a thermostatic water bath in order to maintain a constant temperature (25, 35, or 45°C) and stirring was provided at 200 rpm to ensure that equilibrium was reached. Fig. 6 shows the biosorption of MB by PP. It was found that the biosorption kinetics of basic dye decreased with the increase in temperature (from 25 to 45°C). This indicates that the biosorption process is exothermic in nature. Similar results have been found by Demir et al. [29] and Chandra et al. [44] for the sorption of MB on Luffa cylindrical fibers and activated carbon prepared from durian shell, respectively. As the temperature increases, the physical bonding between the dye molecules and the active sites of the biosorbent weakens. Besides, the solubility of MB also increased which caused the interaction forces between the solute and the solvent to become stronger than solute and sorbent; therefore, the solute was more difficult to be

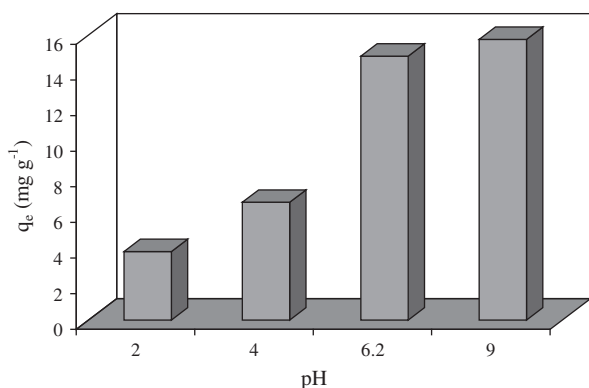


Fig. 5. Effect of pH on the biosorption of MB by PP (conditions: C_0 40 mg L^{-1} ; biosorbent dosage = 0.2 g $(100 \text{ mL})^{-1}$; stirring speed = 200 rpm; $T = 25^\circ\text{C}$).

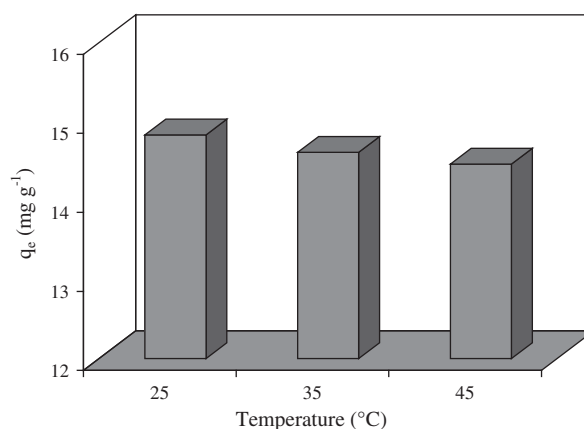


Fig. 6. Effect of temperature on the biosorption of MB by PP (conditions: C_0 40 mg L^{-1} ; biosorbent dosage = 0.2 g $(100 \text{ mL})^{-1}$; stirring speed = 200 rpm; pH 6.2).

adsorbed [45]. In addition, it can be seen that there is no significant effect of temperature on the equilibrium biosorption capacity (Fig. 6), because the amount of MB biosorbed at equilibrium (q_e) decreases slightly from 14.83 to 14.46 mg g⁻¹ with an increase in temperature from 25 to 45°C, respectively.

3.2.4. Effect of biosorbent dose

The mass of biosorbent was varied in the range of 0.20–0.7 g for the removal of MB from aqueous solution by PP, by keeping all other parameters such as initial MB concentration, solution volume, temperature, stirring speed and pH constant. The effect of biosorbent dose on the MB biosorption kinetics by the PP is shown in Fig. 7. The amount of MB biosorbed per unit mass of biosorbent decreases with an increase in biosorbent dose due to the concentration gradient between solute concentrations in the solution and on the biosorbent surface [14]. Thus, with increasing biosorbent dosage, the amount of dye biosorbed by unit weight of biosorbent becomes reduced, thus causing a decrease in biosorption capacity with increasing biosorbent dosage. On the other hand, there is an increase in percentage removal of MB from 63.66 to 91.89% with an increase in PP dosage from 0.2 to 0.7 g (Figure not shown). This can be attributed to increased surface area and the availability of more biosorption sites. A similar phenomenon has been observed for the biosorption of MB on papaya seeds [46].

3.2.5. Effect of ionic strength

In water, salt is present in a wide range of concentrations depending on the source and the quality of the water. The presence of salt or co-ions in solution

can affect the biosorption of dye ions. The effect of ionic strength on the biosorption of MB by PP was studied with a constant initial concentration of 40 mg L⁻¹, biosorbent mass of 0.20 g, solution volume of 100 mL, temperature of 25°C, stirring speed of 200 rpm, and natural pH. The ionic strength of the dye solution was modified using different dosages of NaCl (0.25–2 g (100 mL))⁻¹. Fig. 8 indicates the effect of NaCl concentration (ionic strength) on the removal of MB from aqueous solution by PP. It was observed that the biosorption potential decreased with an increase in concentration of salt (NaCl) in the medium. When the ionic strength was increased, the electrical double layer surrounding the adsorbent surface was compressed, which would lead to a decrease in the electrostatic potential. This indirectly resulted in a reduction of the coulombic free energy, and a decrease in basic dye ions biosorption [47]. Similar results in the literature were found for the biosorption of dyes [14,47–49]. However, these results were unlike those reported by other authors [34,50,51].

3.2.6. Effect of biosorbent particle size

The effect of particle size of PP on the MB removal was studied using three particle size ranges: 0.18–0.5, 0.5–1.25, and 1.25–2 mm, keeping all other parameters constant. Fig. 9 shows the biosorption equilibrium of the dye at three different particle sizes. As can be seen from this figure, the removal is improved as the particle size decreases. This is because the smaller particles have more surface area and access to the particle pores is easier when their size is small. The relationship between the effective surface area of the biosorbent particles and their sizes is that the effective surface area increases as the particle size decreases and as a consequence, the

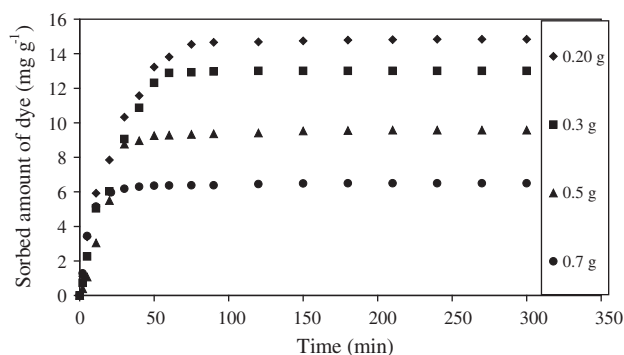


Fig. 7. Effect of dosage biosorbent on the biosorption of MB by PP (conditions: $C_0 = 40 \text{ mg L}^{-1}$; $V = 100 \text{ mL}$; stirring speed = 200 rpm; $T = 25^\circ\text{C}$; pH 6.2).

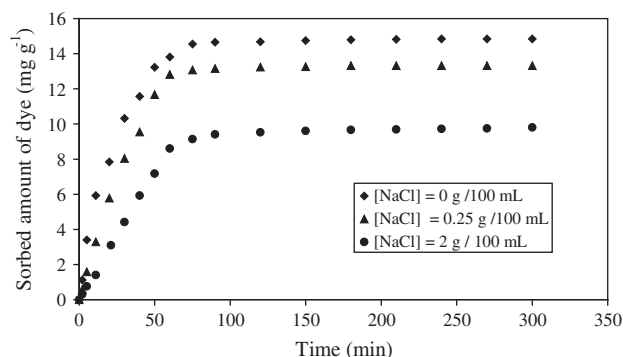


Fig. 8. Effect of ionic strength on the biosorption of MB by PP (conditions: $C_0 = 40 \text{ mg L}^{-1}$; biosorbent dosage = 0.2 g (100 mL)⁻¹; stirring speed = 200 rpm; $T = 25^\circ\text{C}$; pH 6.2).

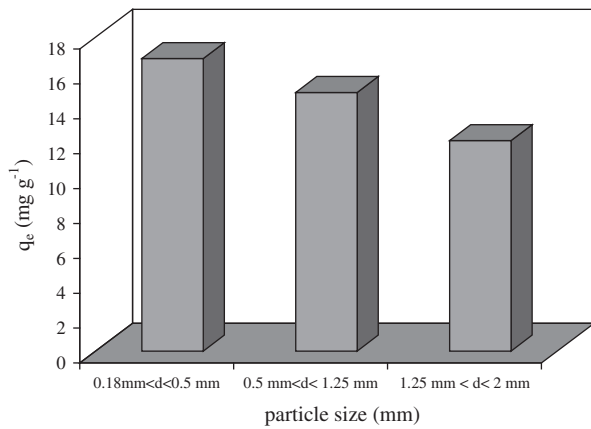


Fig. 9. Effect of biosorbent particle size on the biosorption of MB by PP (conditions: C_0 40 mg L⁻¹; biosorbent dosage = 0.2 g (100 mL)⁻¹; stirring speed = 200 rpm; T = 25 °C; pH 6.2).

biosorption capacity per unit mass of the biosorbent increases. Thus, the smaller PP particle sizes for a given mass of biosorbent have more surface area and therefore the number of available sites is higher. For the biosorption of malachite green by PP [14] and MB by hazelnut shell [34], the biosorption was also found to increase with a decrease in the particle size of biosorbent.

3.3. Biosorption kinetics studies

For a better understanding of biosorption kinetics, various models such as Lagergren's pseudo first-order, Blanchard's pseudo-second-order, Elovich and others kinetic models were used. However, in this study, only two kinetic models were applied for the biosorption of MB by PP at different initial concentrations (from 10 to 40 mg L⁻¹) namely, Lagergren's pseudo-first-order and Blanchard's pseudo-second-order models. The best-fit model was selected based on the linear regression correlation coefficient (r) and values of the biosorbed dye amount (q_e).

The Lagergren's equation was used to investigate the suitability of pseudo-first-order kinetic model and obtain rate constants. This equation can be written as [52]:

$$\ln(q_e - q_t) = \ln q_e - k_1 t \quad (5)$$

where q_e (mg g⁻¹) and q_t (mg g⁻¹) represent the amount of MB biosorbed at equilibrium and at any time t , respectively, and k_1 (min⁻¹) represents the biosorption rate constant.

The value of the biosorption rate constant, k_1 , was determined from the plot of $\ln(q_e - q_t)$ vs. t (figure not

shown). The k_1 values, the correlation coefficients, r , the calculated amount of biosorbed MB ($q_{e,cal}$), and experimental ($q_{e,exp}$) values were collected and are shown in Table 4. It can be seen that Lagergren first-order kinetics equation does not represent a good fit with the experimental data, because the linear regression correlation coefficients (r) are low (0.872–0.932) and the experimental amount of MB biosorbed disagree with calculated values. In many cases, the first-order equation of Lagergren does not fit well to the whole range of contact time and is generally applicable over the initial stage of the adsorption processes [53].

The kinetic data were further analyzed using a pseudo-second-order relation [54]:

$$\frac{dq}{dt} = k_2 (q_e - q_t)^2 \quad (6)$$

Separating the variables in Eq. (6) and integrating this for the boundary conditions $t = 0$ to $t = t$ and $q_t = 0$ to $q_t = q_t$, gives

$$\frac{t}{q_t} = \frac{1}{k_2 q_e^2} + \frac{1}{q_e} t \quad (7)$$

where k_2 (g mg⁻¹ min⁻¹) is the pseudo-second-order rate constant, and q_e and q represent the amount of biosorbed dye (mg g⁻¹) at equilibrium and at any time t .

The constant k_2 is used to calculate the initial biosorption rate h (mg g⁻¹ min⁻¹) as follows:

$$h = k_2 q_e^2 \quad (8)$$

Fig. 10 shows the pseudo-second-order plots for the MB by PP at different concentrations (from 10 to 40 mg L⁻¹) and at 25 °C. The pseudo-second-order rate constants values, and the corresponding linear regression correlation coefficients values (r) are shown in Table 4. It was noticed that, at all initial dye concentrations and for the entire biosorption period, the linear regression correlation coefficient values were found to be higher, and it ranged from 0.997 to 0.999. It was further shown a good agreement between experimental and calculated values. Subsequently, these prove the applicability of this kinetic equation and the pseudo-second-order nature of the biosorption process of MB by PP. Similar kinetic results were already reported by some authors in MB biosorption on various biosorbents [31,34,39,55–57].

Table 4

Parameters of the kinetic models for the biosorption of MB by PP at different concentrations, k_1 (min^{-1}), k_2 ($\text{g mg}^{-1} \text{min}^{-1}$), h ($\text{mg g}^{-1} \text{min}^{-1}$), $q_{e(\text{cal})}$ (mg g^{-1}), $q_{e(\text{exp})}$ (mg g^{-1})

Initial conc (mg L^{-1})	$q_{e,\text{exp}}$	Lagergren pseudo-first-order			Pseudo-second-order			
		k_1	$q_{e,\text{cal}}$	r	k_2	$q_{e,\text{cal}}$	h	r
10	3.92	0.052	1.48	0.872	0.092	3.67	1.24	0.999
20	7.32	0.036	12.85	0.932	0.012	7.32	0.72	0.999
30	11.29	0.029	5.98	0.918	0.005	11.29	0.80	0.997
40	14.83	0.047	19.87	0.890	0.002	15.52	1.34	0.998

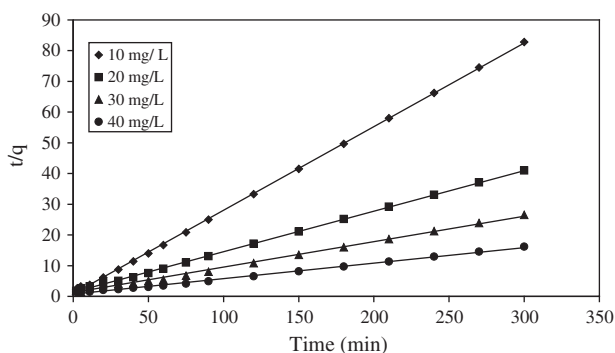


Fig. 10. Pseudo-second-order kinetic for the biosorption of MB by PP.

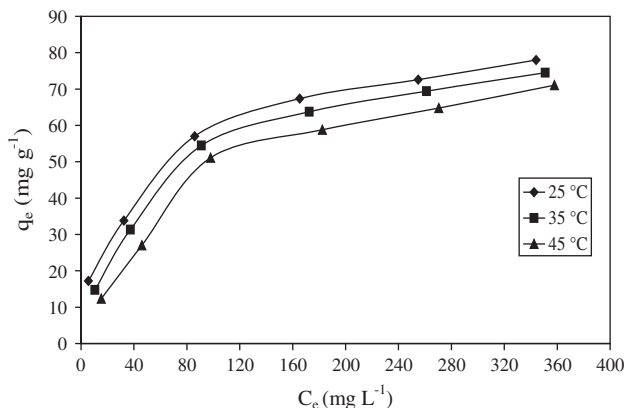


Fig. 11. Equilibrium isotherms of MB biosorption by PP at different temperatures.

3.4. Isotherm modeling

The biosorption isotherm describes the relationship between the amount of sorbate sorbed on the biosorbent and the concentration of dissolved sorbate in the liquid at equilibrium. The equilibrium isotherms at different temperatures (25–45 °C) of MB biosorption by PP are shown in Fig. 11. The trend of the curves q_e vs. C_e , clearly indicated that the isotherms for the three temperatures belong to L type according to the classification of equilibrium isotherm in solution by Giles et al. [58]. The biosorption of MB by PP decreases progressively with the increase in temperature from 25 to 45 °C, as shown in Fig. 11. This indicates that the biosorption process by PP is exothermic. When increasing temperature physical forces responsible of the biosorption decrease [45].

Various isotherm equations have been used to describe the equilibrium data. In the literature, some of these equations are, for instance, Langmuir, Freundlich, Elovich, Flory–Huggins, Harkins–Jura, Dubinin–Radushkevich, Redlich–Peterson, and other isotherm models. In this work, the biosorption equilibrium data of MB by PP were modeled by Langmuir, Freundlich, Elovich, and Flory–Huggins models.

3.4.1. Langmuir model

The Langmuir (1916) model assumes uniform energies of sorption onto the surface and no transmigration of sorbate in the plane [59].

$$q_e = \frac{q_m b C_e}{1 + b C_e} \quad (9)$$

where q_e is the amount of solute sorbed per unit weight of biosorbent at equilibrium (mg g^{-1}), C_e is the equilibrium concentration of the solute in the bulk solution (mg L^{-1}), q_m is the maximum biosorption capacity (mg g^{-1}) and b is the constant related to the free energy of biosorption (L mg^{-1}). The linear form of the Langmuir isotherm is given by the following equation:

$$\frac{C_e}{q_e} = \frac{1}{q_m} C_e + \frac{1}{b \cdot q_m} \quad (10)$$

Fig. 12 presents the linear plot of C_e/q_e vs. C_e . The values of constants q_m , b and the correlation coefficients

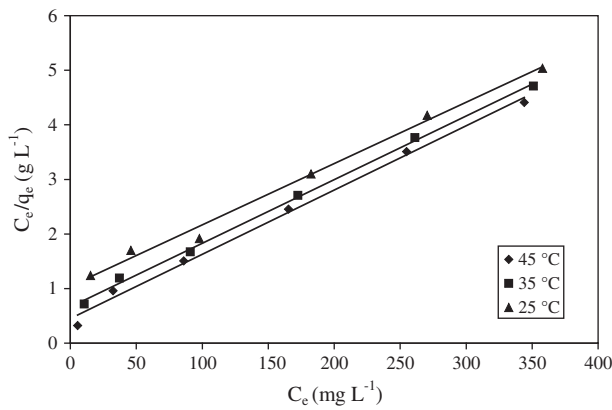


Fig. 12. Langmuir isotherm for the biosorption of MB by PP at different temperatures.

(*r*) were calculated and reported in Table 5. The obtained results show an excellent agreement of the experimental data with the Langmuir equation with good correlation coefficients varying from 0.999 to 0.996 as the temperatures was increased from 25 to 45°C. This good agreement shows uniform energies of biosorption onto the biosorbent surface. The maximum monolayer capacities (*q_m*) obtained are 105.26, 100.02, and 92.59 mg g⁻¹ at 25, 35, and 45°C, respectively.

A further analysis of the Langmuir equation can be made on the basis of a dimensionless equilibrium parameter, *R_L* also known as the separation factor, given by [60]:

$$R_L = \frac{1}{1 + b \times C_0} \tag{11}$$

where *b* is the Langmuir constant and *C₀* is the initial concentration of the sorbate in solution. The value of *R_L* lies between 0 and 1 for favorable adsorption, while *R_L* > 1 represents unfavorable adsorption, and *R_L* = 1 represents linear adsorption while the adsorption process is irreversible if *R_L* = 0. The calculated *R_L* values vs. initial dye concentration at three different temperatures were represented in Fig. 13. From this figure, it was observed that the biosorption of MB by PP was found to be more favorable at lower temperature and at higher concentrations. Also the value of *R_L* in the range of 0–1 at all initial MB concentrations and at the three studied temperatures confirms the favorable uptake of MB process.

3.4.2. Freundlich model

The empirical model can be applied to non-ideal sorption on heterogeneous surfaces as well as multilayer sorption and is expressed by the following equation [61]:

$$q_e = K_F C_e^{1/n} \tag{12}$$

where *n* is a constant of the sorption intensity and *K_F* is a constant of the relative biosorption capacity of the biosorbent (mg^{1-1/n} L^{1/n} g⁻¹). The fit of data to Freundlich isotherm indicates the heterogeneity of the biosorbent surface. The *n* value indicates the degree of non-linearity between solution concentration and adsorption as follows: if *n* = 1, the adsorption is linear; if *n* < 1, the adsorption process is chemical and if *n* > 1, the adsorption is a favorable physical process

Table 5
Parameters of isotherm models for removal of MB by PP at different temperatures

Model	Parameters	T (°C)		
		25	35	45
Langmuir	<i>q_m</i> (mg g ⁻¹)	105.26	100.02	92.59
	<i>b</i> (×10 ³ L mg ⁻¹)	9.93	6.65	4.87
	<i>r</i>	0.999	0.998	0.996
Freundlich	<i>K_F</i> (mg ^{1-1/n} L ^{1/n} g ⁻¹)	9.37	5.50	3.12
	<i>n</i>	2.65	2.15	1.80
	<i>r</i>	0.991	0.981	0.970
Elovich	<i>q_m</i> (mg g ⁻¹)	25.17	33.55	44.64
	<i>K_E</i> (L mg ⁻¹)	0.21	0.06	0.02
	<i>r</i>	0.983	0.975	0.939
Flory–Huggins	<i>K_{FH}</i> (×10 ³ L mg ⁻¹)	4.73	4.28	3.75
	<i>n_{FH}</i>	0.83	0.73	0.58
	<i>r</i>	0.987	0.980	0.962

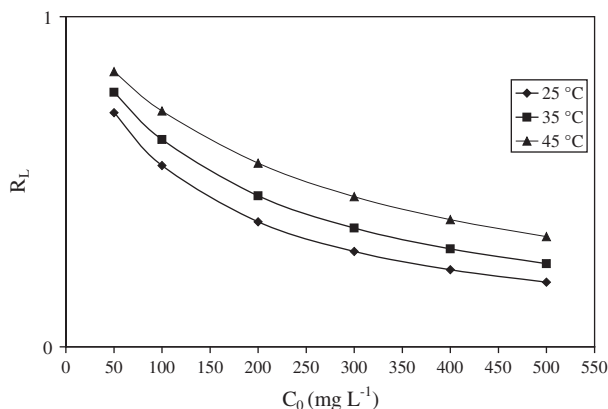


Fig. 13. Separation factor (R_L) for the biosorption of MB by PP at different temperatures.

[62]. Eq. (12) can be linearized in the form of Eq. (13) and the constants can be determined:

$$\ln q_e = \ln K_F + \frac{1}{n} \ln C_e \quad (13)$$

The corresponding Freundlich parameters (K_F , n) and the correlation coefficients (r) are given in Table 5. This result indicates that the Freundlich parameters decrease with an increase of temperature; however, the correlation coefficients obtained are higher and varies between 0.970 and 0.991, but they are lower than those obtained from Langmuir model. The obtained n value $n > 1$, indicates that biosorption of the MB by PP is a favorable physical process.

3.4.3. Elovich isotherm model

This model is based on a kinetic principle assuming that the adsorption sites increase exponentially with adsorption, which implies a multilayer adsorption [63]. It is expressed by the relation [64]:

$$\frac{q_e}{q_m} = K_E C_e \exp\left(-\frac{q_e}{q_m}\right) \quad (14)$$

where K_E is the Elovich equilibrium constant ($L \text{ mg}^{-1}$) and q_m is the Elovich maximum adsorption capacity (mg g^{-1}). The linearized form of the Eq. (14) is given below:

$$\ln \frac{q_e}{C_e} = \ln K_E q_m - \frac{q_e}{q_m} \quad (15)$$

If the biosorption obeys to Elovich equation, Elovich maximum adsorption capacity, q_m , and Elovich

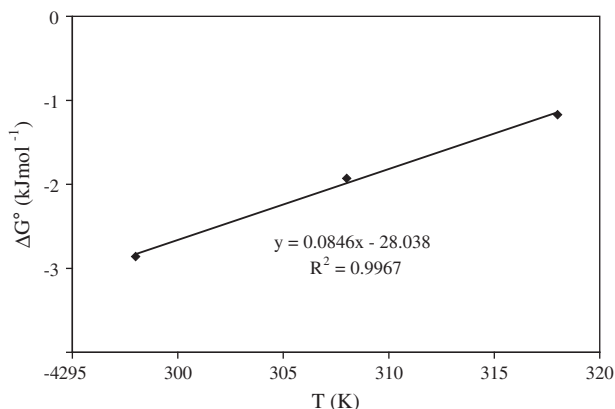


Fig. 14. Plot of ΔG° vs. T for estimation of thermodynamic parameters for the biosorption of MB by PP.

constant, K_E , can be calculated from the slopes and the intercepts, respectively, of the plot $\ln(q_e/C_e)$ vs. q_e . The variables of Elovich (K_E , q_m) and the correlation coefficients (r) values are collected in Table 5. The values of maximum biosorption capacity, and the correlation coefficients indicate that the Elovich model is not suitable to describe the experimental data for the biosorption isotherms of MB by PP.

3.4.4. Flory–Huggins isotherm model

The original Flory–Huggins isotherm describes the behavior of a two-dimensional lattice of non-interacting particles of different sizes [65]:

$$\frac{\theta}{C_0} = K_{FH}(1 - \theta)n^{FH} \quad (16)$$

Eq. (16) can be further transformed to the following linearized form:

$$\ln\left(\frac{\theta}{C_0}\right) = \ln K_{FH} + n_{FH} \ln(1 - \theta) \quad (17)$$

where $\theta = q_e/q_m$ is the degree of surface coverage, K_{FH} is the indication of Flory–Huggins equilibrium

Table 6
Thermodynamic parameters for the biosorption MB

T (°C)	ΔH° (kJ mol ⁻¹)	ΔG° (kJ mol ⁻¹)	ΔS° (J mol ⁻¹ K ⁻¹)
25	-28.03	-2.86	-84.6
35		-1.93	
45		-1.17	

constant which is used for the calculation of spontaneity free Gibbs energy, and n_{FH} is constant model exponent. Flory–Huggins isotherm model [66] can express the feasibility and spontaneous nature of an adsorption process.

If the biosorption data obeys Flory–Huggins model, the constants K_{FH} and n_{FH} can be calculated from the slope and the intercept of the plot $\ln\left(\frac{\theta}{C_0}\right)$ vs. $\ln(1-\theta)$. The corresponding Flory–Huggins parameters and the correlation coefficients are listed in Table 5. Relying upon on the correlation coefficients (r) values obtained that are low (≥ 0.962), these

results confirm that this model was inappropriate to predict the biosorption isotherms of MB by PP. In the literature, Horsfall and Spiff [66] also have used this model to study the equilibrium biosorption of Al^{3+} , Co^{2+} , and Ag^+ by fluted pumpkin waste biomass.

In conclusion, the experimental data for the biosorption isotherms of basic dye, MB, by PP can be better explained by Langmuir model which shows uniform energies of biosorption on the surface. Furthermore, the biosorption of the MB by PP is a favorable physical process.

Table 7

Comparison of maximum monolayer biosorption capacity (q_m) and experimental conditions used of MB biosorption from the literature by various low-cost biosorbents

Low-cost biosorbents	Experimental conditions					
	Initial concentration range (mg L ⁻¹)	pH	T (°C)	Biosorbent dosage (g)	q_m (mg g ⁻¹)	Equilibrium time
PPs [15]	25–400	8	20 ± 1	0.1–1.00	33.55	60 min
Coconut bunch waste [17]	50–500	6.5–7.5	30	0.2	70.92	3–5 h
Guava leaf powder [21]	100–800	7.5	30	2	295	*
Meranti sawdust [23]	50–200	9	30	0.5	120.48	3 h
<i>Luffa cylindrical fibers</i> [29]	10–100	*	30	0.8	47	After 12 h
Sawdust of hazelnut shells [31]	250–1,000	*	20	0.5	76.9	120 min–>180 min
Garlic peel [41]	25–200	4–12	30	0.3	82.64	60 min–>130 min
Rice bran [47]	80	6	20	5	54.99	60 min
Wheat bran [47]	80	6	20	5	16.62	90 min
Fly ash [55]	20–100	8	30	0.6	5.57	After 60 min
Coir pith carbon [56]	10–40	6.9	35	0.3	5.87	(40–120) min
Yellow passion fruit waste [70]	5–600	8	25	0.1–1.00	44.7	48 h
Dehydrated peanut hull [71]	100–400	3.5	30	0.1	123.5	24 h
Coffee husks [72]	50–500	8	30	10	90.09	*
AC of <i>Euphorbia rigida</i> [73]	100–400	6.0	40	2	114.45	60 min
Rice husk [74]	10–100	6.8–7.1	25 ± 2	2	8.07	*
Tomato plant root [75]	100–600	6.67	30	0.25	83.33	15 min
AC of fir wood [76]	200	6.6	30	1.00	70.05	*
AC of <i>cocos nucifera</i> L. [77]	60–100	*	30	0.25	15.59	100 min
AC of oil palm wood [78]	10–250	*	30	0.05	90.9	*
PP in This work	40–400	6.2 (natural)	25	0.1	105.26	(75–480) min

Notes: AC: activated carbon.

*Does not reported.

3.5. Thermodynamic parameters

Thermodynamic parameters are important in biosorption studies for better understanding of temperature effect on biosorption. To determine whether the process will occur spontaneously, a set of thermodynamic parameters for the MB–PP biosorption system were calculated, including Gibbs free energy change (ΔG°), enthalpy change (ΔH°), and entropy change (ΔS°) [14]:

$$\Delta G^\circ = -R_g T \ln b_M \quad (18)$$

$$\Delta G^\circ = \Delta H^\circ - T\Delta S^\circ \quad (19)$$

where T (K) is the absolute temperature and R_g ($8.314 \text{ J mol}^{-1} \text{ K}^{-1}$) is the gas constant, and b_M (L mol^{-1}) is the Langmuir equilibrium constant.

The values of Gibbs free energy change (ΔG°) were obtained according to Eq. (18) at different temperatures. From the slope and the intercept of the plot of ΔG° vs. T as presented in Fig. 14, ΔH° and ΔS° values were estimated. The calculated parameters by using the above equations were collected in Table 6. As can be seen, ΔG° values were obtained to be -2.86 , -1.93 , and $-1.17 \text{ kJ mol}^{-1}$ at 25, 35, and 45°C, respectively. Negative values of Gibbs free energy show the feasibility of the process and the spontaneous nature of biosorption with a high preference of MB by PP. Knowing that generally, the change of free energy for the physical and chemical adsorption is in the range of 0 to -20 kJ/mol and -80 to -400 kJ/mol , respectively [67]. The lower and negative value of ΔS° ($-84.6 \text{ J mol}^{-1} \text{ K}^{-1}$) indicates that it may imply that no remarkable change in entropy during the biosorption of MB and the biosorption process is reversible. Also, the negative value of ΔS° definitely reflects that no significant change occurs in the internal structure of the biosorbent during the biosorption process [68]. The negative value of enthalpy change ($-28.03 \text{ kJ mol}^{-1}$) indicates the exothermic nature of the biosorption interaction. The decrease in biosorption capacity (q_m) with the increase in temperature is due to the weakening of sorptive forces between the active sites on the PP and the dye species, and also between adjacent dye molecules on the biosorbed phase [45]. In brief, the thermodynamic parameters indicate that the biosorption process of MB by PP is spontaneous, physical and exothermic in nature. In the literature, similar thermodynamic results were found for the biosorption of dyes [67,69].

3.6. Evaluation of PP as biosorbent

Table 7 lists a comparison of maximum monolayer biosorption capacity (q_m) of MB by various low-cost biosorbents. This study presents a relatively large maximum monolayer biosorption capacity (105.26 mg g^{-1}) at natural pH and room temperature (25°C). On this basis, we can conclude that PP could be considered an effectual bio-solid as compared with reported low-cost biosorbents for the removal of MB from aqueous media.

4. Conclusions

The results obtained in this study demonstrate PP potential for the removal of MB dye from aqueous media. The PP presents SSA of $167.41 \text{ m}^2 \text{ g}^{-1}$ and pH_{pzc} of 5.7. The concentrations of acid groups were higher than the basic groups and this result determines the nature of the PP surface which improves the biosorption of the basic MB dye from the solution. In addition, the FTIR reveals the main functional groups that might be enhanced in MB biosorption such as OH of phenol group of cellulose and lignin. The SEM of fresh PP sample exhibits that it has a rough and porous surface structure which also improves the biosorption of dye.

The amount of MB biosorbed was found to increase with an increase in the contact time, initial dye concentrations, and the pH. Also, the removal percentage was found to increase with the increase of biosorbent dosage. The contact time required to reach the equilibrium at initial concentrations from 10 to 40 mg L^{-1} is from 20 to 75 min, respectively. However, the amount of MB dye biosorbed decreases with the increase of temperature, ionic strength, and particle size. The experimental data for the biosorption kinetics were found to conform to pseudo-second-order kinetics with a good correlation. Equilibrium data were best described by Langmuir isotherm model, confirming the monolayer biosorption capacity of MB by PP with a monolayer biosorption capacity of 105.26 mg g^{-1} . The dimensionless separation factor (R_L) showed that PP could be used for removal of MB from aqueous media. The data obtained from biosorption isotherms at different temperatures were used to determine thermodynamic parameters such as ΔG° , ΔH° , and ΔS° of biosorption. The results suggest that the biosorption is a physical process, spontaneous and exothermic in nature.

Consequently, the results of this study will be useful for using this agricultural waste as an economic

biosorbent (biomaterial) for basic dyes removal in wastewater treatment process since it is available in large amounts. Additionally, the biosorbent shows higher maximum monolayer biosorption capacity and specific surface area than other agricultural wastes which were investigated by other researchers.

Acknowledgments

The authors acknowledge the research grant provided by the Ministry of Higher Education and Scientific Research of Algeria. The authors thank Mr. Fadel Ismail for his assistance in FTIR analysis.

References

- [1] E.A. Clarke, R. Anliker, Organic dyes and pigments, in: O. Hutzinger (Ed.), Handbook of Environmental Chemistry, vol. 3, part A: Anthropogenic Compounds, Springer-Verlag, Heidelberg, 3 (1980) 181–215.
- [2] H. Zollinger, Azo Dyes and Pigments. Color Chemistry: Synthesis, Properties and Applications of Organic Dyes and Pigments, VCH, New York, NY, 1987.
- [3] P.K. Malik, Use of activated carbon prepared from sawdust and rice-husk for adsorption of acid dyes: A case study of Yellow 36, Dyes Pigm. 56 (2003) 39–49.
- [4] G. Crini, Non-conventional low-cost adsorbents for dye removal: A review, Bioresour. Technol. 97 (2006) 1061–1085.
- [5] K.G. Bhattacharyya, A. Sharma, Kinetics and thermodynamics of methylene blue adsorption on neem (*Azadirachta indica*) leaf powder, Dyes Pigm. 65 (2005) 51–59.
- [6] M. Goyal, S. Singh, R.C. Bansal, Equilibrium and dynamic adsorption of methylene blue from aqueous solutions by surface modified activated carbons, Carbon Sci. 5 (2004) 70–79.
- [7] F.K. Bangash, A. Manaf, Kinetics of removal of dye (Basic blue 3) from aqueous solution by activated charcoal from the wood of *Braunsonitia papyrifera* (*Paper mulberry*), J. Chem. Soc. Pakistan 26 (2004) 111–115.
- [8] E. Lorenc-Grabowska, G. Gryglewicz, Adsorption characteristics of Congo Red on coal-based mesoporous activated carbon, Dyes Pigm. 68 (2006) 1–7.
- [9] C. Namasivayam, D. Kavita, Removal of Congo Red from water by adsorption onto activated carbon prepared from coir pith, an agricultural solid waste, Dyes Pigm. 54 (2002) 47–58.
- [10] R.L. Teng, F.C. Wu, R.S. Juang, Liquid-phase adsorption of dyes and phenols using pine wood-based activated carbons, Carbon 41 (2003) 487–495.
- [11] B.H. Hameed, A.T.M. Din, A.L. Ahmad, Adsorption of methylene blue onto bamboo-based activated carbon: Kinetics and equilibrium studies, J. Hazard. Mater. 141 (2007) 819–825.
- [12] I.A.W. Tan, B.H. Hameed, A.L. Ahmad, Equilibrium and kinetic studies on basic dye adsorption by oil palm fibre activated carbon, Chem. Eng. J. 127 (2007) 111–119.
- [13] B.H. Hameed, A.L. Ahmad, K.N.A. Latiff, Adsorption of basic dye (methylene blue) onto activated carbon prepared from rattan sawdust, Dyes Pigm. 75 (2007) 143–149.
- [14] E.K. Guechi, O. Hamdaoui, Sorption of malachite green from aqueous solution by potato peel: Kinetics and equilibrium modeling using non-linear analysis method, Arab. J. Chem. (2011), doi: 10.1016/j.arabjc.2011.05.011.
- [15] Y.A. Oktem, S.G. Pozan Soyly, N. Aytan, The adsorption of methylene blue from aqueous solution by using waste potato peels; equilibrium and kinetic studies, J. Sci. Ind. Res. 71 (2012) 817–821.
- [16] P.S. Rao, K.V.N.S. Reddy, S. Kalyani, A. Krishnaiah, Comparative sorption of copper and nickel solutions by natural neem (*Azadirachta indica*) sawdust and acid treated sawdust wood, Sci. Technol. 41 (2007) 427–442.
- [17] B.H. Hameed, D.K. Mahmoud, A.L. Ahmad, Equilibrium modeling and kinetic studies on the adsorption of basic dye by a low-cost adsorbent: Coconut (*Cocos nucifera*) bunch waste, J. Hazard. Mater. 158 (2008) 65–72.
- [18] H.P. Boehm, Chemical identification of surface groups, Adv. Catal. 16 (1966) 179–274.
- [19] L.S. Balistrieri, J.W. Murray, The surface chemistry of goethite (α -FeOOH) in major ion seawater, Am. J. Sci. 281 (1981) 788–806.
- [20] H. Deng, L. Yang, G. Tao, J. Dai, Preparation and characterization of activated carbon from cotton stalk by microwave assisted chemical activation—Application in methylene blue adsorption from aqueous solution, J. Hazard. Mater. 166 (2009) 1514–1521.
- [21] V. Ponnusami, S. Vikram, S.N. Srivastava, Guava (*Psidium guajava*) leaf powder: Novel adsorbent for removal of methylene blue from aqueous solutions, J. Hazard. Mater. 152 (2008) 276–286.
- [22] M. Khormaei, B. Nasernejad, M. Edrisi, T. Eslamzadeh, Copper biosorption from aqueous solutions by sour orange residue, J. Hazard. Mater. 149 (2007) 269–480.
- [23] A. Ahmad, M. Rafatullah, O. Sulaiman, M.H. Ibrahim, R. Hashim, Scavenging behaviour of meranti sawdust in the removal of methylene blue from aqueous solution, J. Hazard. Mater. 170 (2009) 357–365.
- [24] M. Auta, B.H. Hameed, Preparation of waste tea activated carbon using potassium acetate as an activating agent for adsorption of Acid Blue 25 dye, Chem. Eng. J. 171 (2011) 502–509.
- [25] L.S. Silva, L.C.B. Lima, F.C. Silva, J.M.E. Matos, M.R.M.C. Santos, L.S.S. Junior, K.S. Sousa, E.C. Silva Filho, Dye anionic sorption in aqueous solution onto a cellulose surface chemically modified with amino ethanethiol, Chem. Eng. J. 218 (2013) 89–98.
- [26] B.H. Hameed, M.I. El-Khaiary, Batch removal of malachite green from aqueous solutions by adsorption on oil palm trunk fibre: Equilibrium isotherms and kinetic studies, J. Hazard. Mater. 154 (2008) 237–244.
- [27] T.S. Anirudhan, P. Senan, M.R. Unnithan, Sorptive potential of a cationic exchange resin of carboxyl banana stem for mercury (II) from aqueous solutions, Sep. Purif. Technol. 52 (2007) 512–519.

- [28] G. Annadurai, S.R. Juang, J.D. Lee, Use of cellulose-based wastes for adsorption of dyes from aqueous solutions, *J. Hazard. Mater.* 92 (2002) 263–274.
- [29] H. Demir, A. Top, D. Balkose, S. Ulku, Dye adsorption behavior of *Luffa* cylindrical fibers, *J. Hazard. Mater.* 153 (2008) 389–394.
- [30] V.J.P. Poots, G. McKay, J.J. Hzaly, The removal of acid dye from effluent using natural adsorbant—I PEAT, *Water Res.* 10 (1976) 1061–1066.
- [31] F. Ferrero, Dye removal by low cost adsorbents: Hazelnut shells in comparison with wood sawdust, *J. Hazard. Mater.* 142 (2007) 144–152.
- [32] H. Pekkuz, I. Uzun, F. Guze, Kinetics and thermodynamics of the adsorption of some dyestuffs from aqueous solution by poplar sawdust, *Bioresour. Technol.* 99 (2008) 2009–2017.
- [33] P. Janos, H. Buchtova, M.R. yznarova, Sorption of dyes from aqueous solutions onto fly ash, *Water Res.* 37 (2003) 4938–4944.
- [34] M. Dogan, H. Abak, M. Alkan, Adsorption of methylene blue onto hazelnut shell: Kinetics, mechanism and activation parameters, *J. Hazard. Mater.* 164 (2009) 172–181.
- [35] C. Kaewprasit, E. Hequet, N. Abidi, J.P. Gourolot, Application of methylene blue adsorption to cotton fiber specific surface area measurement. Part I. Methodology, *J. Cotton Sci.* 2 (1998) 164–173.
- [36] C.H. Weng, Adsorption characteristics of new coccine dye onto sludge ash, *Adsorpt. Sci. Technol.* 20 (2002) 669–681.
- [37] V.J.P. Poots, G. McKay, J.J. Healy, The removal of acid dye from effluent using natural adsorbents-II Wood, *Water Res.* 10 (1976) 1067–1070.
- [38] R. Han, W. Zou, W. Yu, S. Cheng, Y. Wang, J. Shi, Biosorption of methylene blue from aqueous solution by fallen phoenix tree's leaves, *J. Hazard. Mater.* 141 (2007) 156–162.
- [39] Y. Bulut, H. Aydın, A kinetics and thermodynamics study of methylene blue adsorption on wheat shells, *Desalination* 194 (2006) 259–267.
- [40] N.A. Oladoja, C.O. Aboluwoye, Y.B. Oladimeji, A.O. Ashogbon, I.O. Otemuyiwa, Studies on castor seed shell as a sorbent in basic dye contaminated wastewater remediation, *Desalination* 227 (2008) 190–203.
- [41] B.H. Hameed, A.A. Ahmad, Batch adsorption of methylene blue from aqueous solution by garlic peel, an agricultural waste biomass, *J. Hazard. Mater.* 164 (2009) 870–875.
- [42] S. Senthilkumaar, P.R. Varadarajan, K. Porkodi, C.V. Subbhuraam, Adsorption of methylene blue onto jute fiber carbon: Kinetics and equilibrium studies, *J. Colloid Interface Sci.* 284 (2005) 78–82.
- [43] V. Vadivelan, K.V. Kumar, Equilibrium, kinetics, mechanism, and process design for the sorption of methylene blue onto rice husk, *J. Colloid Interface Sci.* 286 (2005) 90–100.
- [44] T.C. Chandra, M.M. Mirna, Y. Sudaryanto, S. Ismadji, Adsorption of basic dye onto activated carbon prepared from durian shell: Studies of adsorption equilibrium and kinetics, *Chem. Eng. J.* 127 (2007) 121–129.
- [45] I.A.W. Tan, A.L. Ahmad, B.H. Hameed, Adsorption of basic dye on high-surface-area activated carbon prepared from coconut husk: Equilibrium, kinetic and thermodynamic studies, *J. Hazard. Mater.* 154 (2008) 337–346.
- [46] B.H. Hameed, Evaluation of papaya (*Carica papaya* L.) seeds as a novel non-conventional low-cost adsorbent for removal of methylene blue, *J. Hazard. Mater.* 162 (2009) 939–944.
- [47] X.S. Wang, Y. Zhou, Y. Jiang, C. Sun, The removal of basic dyes from aqueous solutions using agricultural by-products, *J. Hazard. Mater.* 157 (2008) 374–385.
- [48] E.K. Guechi, O. Hamdaoui, Cattail leaves as a novel biosorbent for the removal of malachite green from liquid phase: Data analysis by non-linear technique, *Desalin. Water Treat.* 51 (2013) 3371–3380.
- [49] C.H. Weng, Y.T. Lin, T.W. Tzeng, Removal of methylene blue from aqueous solution by adsorption onto pine apple leaf powder, *J. Hazard. Mater.* 170 (2009) 417–424.
- [50] J. German-Heins, M. Flury, Sorption of brilliant blue FCF in soils as affected by pH and ionic strength, *Geoderma* 97 (2000) 87–101.
- [51] Y. Guo, S. Yang, W. Fu, J. Qi, R. Li, Z. Wang, H. Xu, Adsorption of malachite green on micro- and mesoporous rice husk-based active carbon, *Dyes Pigm.* 56 (2003) 219–229.
- [52] S. Lagergren, About the theory of so-called adsorption of soluble substances, *K. Sven. Vetenskapskad. Handl.* 24 (1898) 1–39.
- [53] G. McKay, Y.S. Ho, The sorption of lead (II) on peat, *Water Res.* 33 (1999) 578–584.
- [54] G. McKay, Y.S. Ho, Pseudo-second order model for sorption processes, *Process Biochem.* 34 (1999) 451–465.
- [55] K.V. Kumar, V. Ramamurthi, S. Sivanesan, Modeling the mechanism involved during the sorption of methylene blue onto fly ash, *J. Colloid Interface Sci.* 284 (2005) 14–21.
- [56] D. Kavitha, C. Namasivayam, Experimental and kinetic studies on methylene blue adsorption by coir pith carbon, *Bioresour. Technol.* 98 (2007) 14–21.
- [57] O. Hamdaoui, Batch study of liquid-phase adsorption of methylene blue using cedar sawdust and crushed brick, *J. Hazard. Mater.* 135 (2006) 264–273.
- [58] C.H. Giles, T.H.M. Ewan, S.N. Nakhwa, D.A. Smith, System of classification of solution adsorption isotherms and its use in diagnosis of adsorption of mechanisms and in measurements of specific surface area of solids, *J. Chem. Soc.* 10 (1960) 3973–3993.
- [59] Langmuir, The constitution and fundamental properties of solids and liquids, *J. Am. Chem. Soc.* 38 (2000) 2221–2295.
- [60] M. Ajmal, R.A.K. Rao, M.A. Khan, Adsorption of Cu from aqueous solution on *Brassica cumpestris* (mustard cake), *J. Hazard. Mater.* 122 (2005) 177–183.
- [61] H.M.F. Freundlich, Over the adsorption in solution, *J. Phys. Chem.* 57 (1906) 385–470.
- [62] G. McKay, H.S. Blair, J.R. Gardner, Adsorption of dyes on chitin-1: Equilibrium studies, *J. Appl. Polym. Sci.* 27 (1982) 3043–3057.
- [63] S.Y. Elovich, O.G. Larinov, Theory of adsorption from solutions of non electrolytes on solid (I) equation adsorption from solutions and the analysis of its simplest form, (II) verification of the equation of adsorption isotherm from solutions, *Izv. Akad. Nauk. SSSR, Otd. Khim. Nauk* 2 (1962) 209–216.

- [64] O. Hamdaoui, E. Naffrechoux, Modeling of adsorption isotherms of phenol and chlorophenols onto granular activated carbon part I. Two-parameter models and equations allowing determination of thermodynamic parameters, *J. Hazard. Mater.* 147 (2007) 381–394.
- [65] Y. Liu, Y.J. Liu, Review, biosorption isotherms, kinetics and thermodynamics, *Sep. Purif. Technol.* 61 (2008) 229–242.
- [66] M. Horsfall, A.I. Spiff, Equilibrium sorption study of Al^{3+} , Co^{2+} and Ag^{2+} in aqueous solutions by fluted pumpkin (*Telfairia occidentalis* HOOK) waste biomass, *Acta Chim. Slov.* 52 (2005) 174–181.
- [67] A. Ozer, G. Akkaya, M. Turabik, Biosorption of Acid Blue 290 (AB 290) and Acid Blue 324 (AB324) dyes on *Spirogyra rhizopus*, *J. Hazard. Mater.* 135 (2006) 355–364.
- [68] T.S. Anirudhan, P.G. Radhakrishnan, Thermodynamics and kinetics of adsorption of Cu(II) from aqueous solutions onto a new cation exchanger derived from tamarind fruit shell, *J. Chem. Thermodyn.* 40 (2008) 702–709.
- [69] S.D. Khattri, M.K. Singh Colour removal from synthetic dye wastewater using a bioadsorbent, *Water Air Soil Pollut.* 120 (2000) 283–294.
- [70] F.A. Pavan, E.C. Lima, S.L.P. Dias, A.C. Mazzocato, Methylene blue biosorption from aqueous solutions by yellow passion fruit waste, *J. Hazard. Mater.* 150 (2008) 703–712.
- [71] D. Ozer, G. Dursun, A. Ozer, Methylene blue adsorption from aqueous solution by dehydrated peanut hull, *J. Hazard. Mater.* 144 (2007) 171–179.
- [72] L.S. Oliveira, A.S. Franca, T.M. Alves, S.D.F. Rocha, Evaluation of untreated coffee husks as potential biosorbents for treatment of dye contaminated waters, *J. Hazard. Mater.* 155 (2008) 507–512.
- [73] O. Gerçel, A. Ozcan, A. Safa Ozcan, H. Ferdi Gerçel, Preparation of activated carbon from a renewable bio-plant of *Euphorbia rigida* by H_2SO_4 activation and its adsorption behavior in aqueous solutions, *Appl. Surf. Sci.* 253 (2007) 4843–4852.
- [74] M. Topcu Sulak, H. Cengiz Yatmaz, Removal of textile dyes from aqueous solutions with eco-friendly biosorbent, *Desalin. Water Treat.* 37 (2012) 169–177.
- [75] C. Kannan, N. Buvanewari, T. Palvannan, Removal of plant poisoning dyes by adsorption on tomato plant root and green, carbon from aqueous solution and its recovery, *Desalination* 249 (2009) 1132–1138.
- [76] F.C. Wu, R.L. Tseng, R.S. Juang, Preparation of highly microporous carbons from fir wood by KOH activation for adsorption of dyes and phenols from water, *Sep. Purif. Technol.* 47 (2005) 10–19.
- [77] Y.C. Sharma, Uma, A.S.K. Sinha, S.N. Upadhyay, Characterization and adsorption studies of *Cocos nucifera* L. Activated carbon for the removal of methylene blue from aqueous solutions, *J. Chem. Eng.* 55 (2010) 2662–2667.
- [78] T.A. Khan, V.V. Singh, D. Kumar, Removal of some basic dyes from artificial textile wastewater by adsorption on Akash Kinari coal, *J. Sci. Ind. Res.* 63 (2004) 355–364.